ACSNANO

www.acsnano.org

ARTICLE

Co-delivery of Peptide Neoantigens and Stimulator of Interferon Genes Agonists Enhances Response to Cancer Vaccines

Daniel Shae,◆ Jessalyn J. Baljon,◆ Mohamed Wehbe, Plamen P. Christov, Kyle W. Becker, Amrendra Kumar, Naveenchandra Suryadevara, Carcia S. Carson, Christian R. Palmer, Frances C. Knight, Sebastian Joyce, and John T. Wilson*

Cite This: *ACS Nano* 2020, 14, 9904–9916

Read Online

ACCESS | Metrics & More | Article Recommendations | Supporting Information

ABSTRACT: **Cancer vaccines targeting patient-specific neoantigens have emerged as a promising strategy for improving responses to immune checkpoint blockade. However, neoantigenic peptides are poorly immunogenic and inept at stimulating CD8$^+$ T cell responses, motivating a need for new vaccine technologies that enhance their immunogenicity. The stimulator of interferon genes (STING) pathway is an endogenous mechanism by which the innate immune system generates an immunological context for priming and mobilizing neoantigen-specific T cells. Owing to this critical role in tumor immune surveillance, a synthetic cancer nanovaccine platform (nanoSTING-vax) was developed that mimics immunogenic cancer cells in its capacity to efficiently promote co-delivery of peptide antigens and the STING agonist, cGAMP. The co-loading of cGAMP and peptides into pH-responsive, endosomolytic polymersomes promoted the coordinated delivery of both cGAMP and peptide antigens to the cytosol, thereby eliciting inflammatory cytokine production, co-stimulatory marker expression, and antigen cross-presentation. Consequently, nanoSTING-vax significantly enhanced CD8$^+$ T cell responses to a range of peptide antigens. Therapeutic immunization with nanoSTING-vax, in combination with immune checkpoint blockade, inhibited tumor growth in multiple murine tumor models, even leading to complete tumor rejection and generation of durable antitumor immune memory. Collectively, this work establishes nanoSTING-vax as a versatile platform for enhancing immune responses to neoantigen-targeted cancer vaccines.**

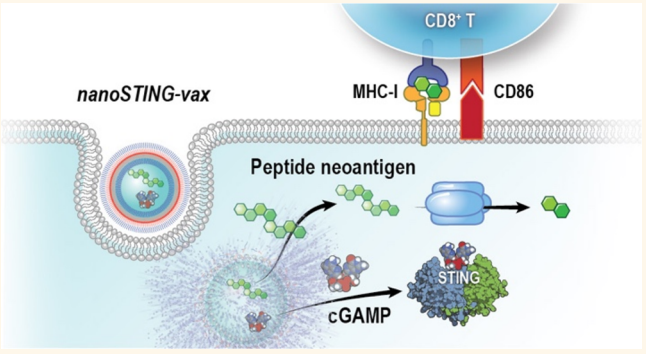

KEYWORDS: *neoantigen, cancer vaccine, immune checkpoint blockade, immunotherapy, polymer nanoparticle*

Immune checkpoint inhibitors are transforming the treatment of an expanding number of tumor types, yet immune checkpoint blockade still benefits only a minority of cancer patients.[1,2] While resistance to immune checkpoint blockade is complex and multifaceted,[3] poor clinical responses can, in part, be ascribed to an insufficient number and/or poor function of endogenously generated, pre-existing T cells that recognize tumor antigens.[4−6] This challenge has created an urgent need for new strategies to bolster the magnitude, breadth, and quality of the antitumor T cell response, including a revitalized interest in therapeutic cancer vaccines.[7−10] While the clinical impact of cancer vaccines over the past several decades has been largely disappointing,[11] the discovery that neoantigens—peptides derived from cancer-specific mutations—are the primary antigenic targets for antitumor T cells has fueled a revolution in the development of personalized cancer vaccines targeting patient-specific mutanomes.[12] Mutations unique to an individual's cancer are identified *via* whole exosome sequencing, advanced immunopeptidomic methods are employed to determine which mutations are most likely to generate neoepitopes, and neoantigenic peptides are then synthesized and administered to the patient as a personalized vaccine product. Peptide antigens, however, are typically

Received: April 1, 2020
Accepted: July 23, 2020
Published: July 23, 2020

https://dx.doi.org/10.1021/acsnano.0c02765
ACS Nano 2020, 14, 9904–9916

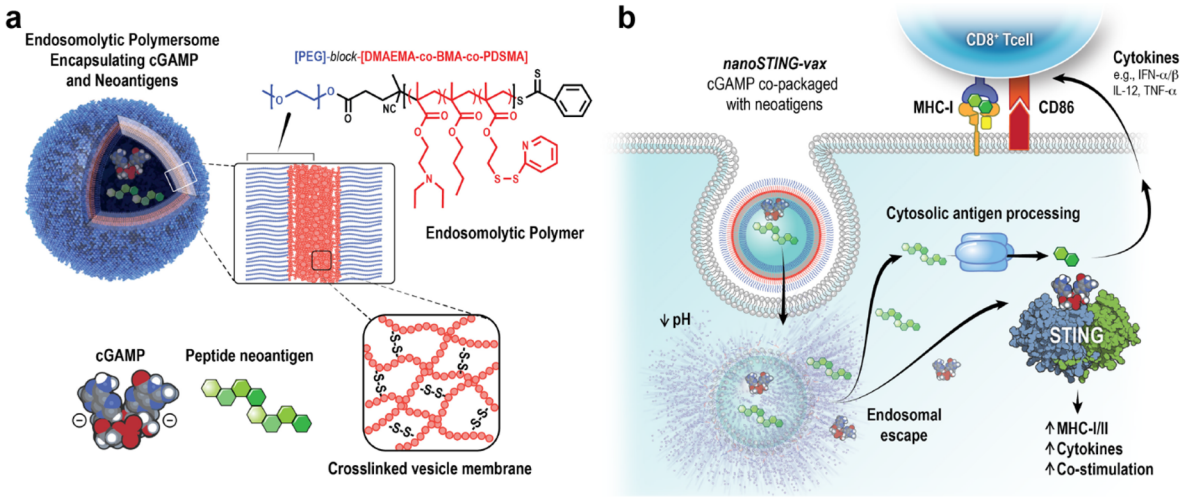

Figure 1. NanoSTING-vax: A platform for dual delivery of peptide antigens and CDN STING agonists to enhance responses to neoantigen-targeted cancer vaccines. (a) Schematic of nanoSTING-vax structure. Peptide antigens and CDN STING agonists (*e.g.*, cGAMP) are co-loaded into pH-responsive polymersomes comprised of endosomolytic diblock polymers. (b) NanoSTING-vax enables uptake of peptides and cGAMP by APCs and facilitates cytosolic co-delivery of neoantigenic peptides and cGAMP *via* endosomal escape. Cytosolic delivery of antigen promotes MHC class I presentation, while cytosolic cGAMP delivery enhances its immunostimulatory adjuvant capacity, collectively resulting in enhanced CD8$^+$ T cell priming and activation. Illustration © 2020, Fairman Studios, LLC.

weakly immunogenic, and, consequently, many cancer vaccine formulations being explored clinically do not elicit robust tumor antigen-specific CD8$^+$ T cell responses, which are critical for effective antitumor immunity.[13,14] This can be mostly attributed to several interrelated barriers, including inefficient accumulation in vaccine site draining lymph nodes (LNs), poor intracellular uptake by antigen presenting cells (APCs), low levels of antigen cross-presentation, and suboptimal choice and/or delivery of immunostimulatory adjuvants.[7,15] This long-standing challenge in synthetic vaccine design has motivated the development of a wide-range of materials-based strategies (*e.g.*, nanoparticles, microparticles, scaffolds, hydrogels) to augment cellular immunity to protein and peptide antigens.[16−18] However, despite these advances, there has been relatively little investigation into the design of particle-based platforms for enhancing the performance of neoantigen-targeted cancer vaccines for personalized immunotherapy.[19−24]

The stimulator of interferon genes (STING) pathway plays a critical role in initiating and propagating endogenous mechanisms of antitumor T cell immunity.[25−27] Upon activation by 2′,5′-3′5′-cyclic guanosine monophosphate-adenosine monophosphate (cGAMP), STING triggers a type-I interferon (IFN-I)-driven inflammatory response that stimulates dendritic cell (DC) cross-presentation of tumor antigens, leading to mobilization of tumor-specific CD8$^+$ T cells. This indispensable role for STING in cancer immune surveillance has recently motivated the study of cGAMP and related cyclic dinucleotides (CDN) as cancer vaccine adjuvants to more closely replicate the natural inflammatory cues that underlie and drive generation of antitumor immunity.[28−32] Notably, Fu *et al.* demonstrated the capacity of STING agonists to enhance immune responses to an autologous cancer cell vaccine,[28] and Kinkead *et al.* have recently leveraged CDNs as an adjuvant in a pancreatic cancer vaccine.[29] While such preclinical studies highlight the potential of STING agonists as cancer vaccine adjuvants, they have co-delivered antigens and CDN adjuvants as a soluble mixture. This formulation strategy has been widely demonstrated to yield less potent and effective immune responses relative to the use of particle-based carriers that mimic pathogens through their capacity to promote the co-delivery of antigen and adjuvant.[33,34] This challenge is further exacerbated by the high water solubility, low molecular weight, and poor drug-like properties of CDNs, which results in their rapid clearance from the injection site with minimal accumulation in the draining LN and inefficient intracellular uptake by APCs,[35−39] critical processes that underlie effective antigen-specific T cell activation. To overcome these barriers, several groups have developed nanocarrier platforms to enhance the intracellular delivery of CDNs, including several liposomal carriers,[40−44] polymeric systems,[45,46] and inorganic nanostructures.[47] Our group has recently described the development of polymer vesicles (polymersomes) with pH-responsive, membrane-destabilizing activity that enhance intracellular uptake and cytosolic delivery of CDNs, resulting in a dramatic enhancement in their immunostimulatory activity.[38] At physiologic pH, the membrane-destabilizing block is sequestered in the polymersome bilayer, shielded by a poly(ethylene glycol) corona. Upon endocytosis and endosomal acidification, the nanoparticles rapidly disassemble to reveal the membrane-interactive segments, resulting in the release of CDNs into the cytosol. Here, we leverage this technology for the development of nanoSTING-vax, a platform for neoantigen-targeted cancer vaccines based on endosomolytic nanoparticles designed to enhance and coordinate the intracellular delivery of neoantigenic peptides and CDN STING agonists (Figure 1). Using synthetic long peptide antigens containing neoepitopes, we demonstrate that nanoSTING-vax can promote the dual delivery of peptides and CDNs to the cytosol, resulting in enhanced antigen cross-presentation and DC maturation, while also promoting accumulation in the vaccine site draining LN. Consequently, nanoSTING-vax enhanced the CD8$^+$ T cell responses to a diversity of peptide antigens, resulting in a dramatic improvement in the response to immune checkpoint blockade in two murine tumor models.

https://dx.doi.org/10.1021/acsnano.0c02765
ACS Nano 2020, 14, 9904−9916

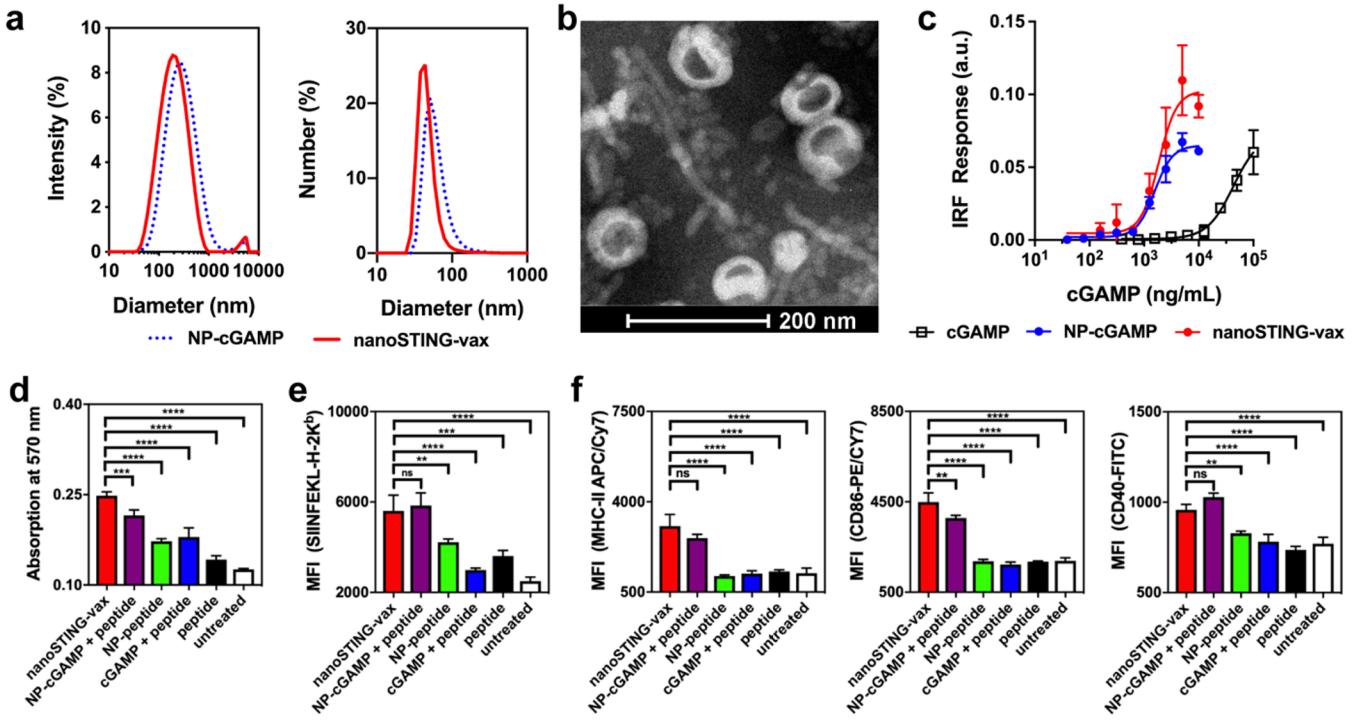

Figure 2. Endosomolytic nanoparticles enhance dual-delivery of cGAMP and peptide antigens to the cytosol. (a) Dynamic light scattering analysis (intensity and number-average size distributions) of cGAMP-loaded polymersomes (NP-cGAMP) and polymersomes loaded with both cGAMP and the Ova-derived peptide SGLEQLESIINFEKL (nanoSTING-vax). (b) Representative transmission electron micrograph of nanoSTING-vax, here loaded with cGAMP and the peptide SGLEQLESIINFEKL. (c) Dose−response curves of the IFN-I response elicited by indicated cGAMP-containing formulations in RAW 264.7 cells with an IFN regulatory factor (IRF)-inducible reporter construct (n = 3 biologically independent samples). (d) B3Z T cell response to DC2.4 DCs treated with the indicated formulation (n = 4 biologically independent samples). (e) Flow cytometric analysis of median fluorescent intensity (MFI) of BMDCs treated with the indicated formulation and stained with an antibody (25-D1.16) specific to the SIINFEKL/H-2K^b complex (n = 3 biologically independent samples). (f) Flow cytometric quantification (MFI) of MHC-II, CD86, and CD40 expression by BMDCs treated with indicated formulation (n = 3 biologically independent samples). Statistical data are presented as mean ± SD. Statistical significance between nanoSTING-vax and all other formulations are shown; $^{**}P < 0.01$, $^{***}P < 0.001$, $^{****}P < 0.0001$ by one-way ANOVA with Tukey posthoc test.

RESULTS AND DISCUSSION

Inspired by endogenous mechanisms of antitumor T cell immunity,[26,27,48−50] we sought to develop a vaccine platform that mimicked an immunogenic cancer cell based on the reductionistic design concept of a vesicular particle encapsulating both peptide antigens and cGAMP (Figure 1a). To accomplish this, we leveraged pH-responsive, endosomolytic polymer vesicles (*i.e.*, polymersomes) previously described by our group that enable the efficient cytosolic delivery of cGAMP.[38] We hypothesized that this class of neoantigen-targeted vaccine, referred to herein as nanoSTING-vax, could enhance tumor antigen-specific T cell responses and, therefore, mitigate resistance to immune checkpoint inhibitors, *via* several mechanisms. First, nanoparticle co-delivery of cGAMP and peptide neoantigen increases the probability that both antigen and adjuvant are delivered to the same APC, allowing antigen processing and presentation to occur in an appropriate pro-inflammatory context, while minimizing the potential for T cell anergy or tolerance due to antigen presentation by immature APCs.[51,52] Second, polymersomes are designed to promote efficient endosomal escape of cargo to the cytosol, allowing cGAMP to access STING while also promoting cytosolic antigen delivery and processing *via* the classical MHC-I antigen presentation pathway (Figure 1b), which has been shown to enhance priming of antigen-specific CD8$^+$ T cells.[53,54] Finally, polymersomes have the potential to enhance LN accumulation and uptake by APCs due to their nanoscale properties.[55]

Co-loading of a bisphosphorothioate analog of cGAMP and six unique peptide sequences, ranging from 9 to 27 amino acids, into polymersomes had no or minimal impact on the size (Figure 2a; Figure S1a) or neutral ζ potential (Figure S1b) of self-assembled particles, which transmission electron microscopy revealed were predominantly of vesicular morphology, though micelles and filamentous structures were also observed (Figure 2b; Figure S2), species that we have previously demonstrated are inefficient at enhancing cGAMP delivery.[38] Importantly, the potent STING activation that we have previously described can be achieved *via* loading of cGAMP into endosomolytic nanoparticles was maintained when both peptides and cGAMP were co-loaded into polymersomes (Figure 2c; Figure S1c). Notably, peptides of variable length, charge, and hydrophobicity could be loaded into polymersomes, albeit with variable encapsulation efficiency (Table S1). Interestingly, we observed a statistically significant correlation between peptide hydrophobicity and loading efficiency (Figure S3), potentially reflecting a preferential association of peptides with the vesicle membrane or aqueous core during the self-assembly process based on their relative water solubility. Hence, the biphasic structure inherent to polymersomes may offer an important advantage for the delivery of peptide neoantigens, which are inherently personalized and, therefore, span a wide range of properties.

https://dx.doi.org/10.1021/acsnano.0c02765
ACS Nano 2020, 14, 9904−9916

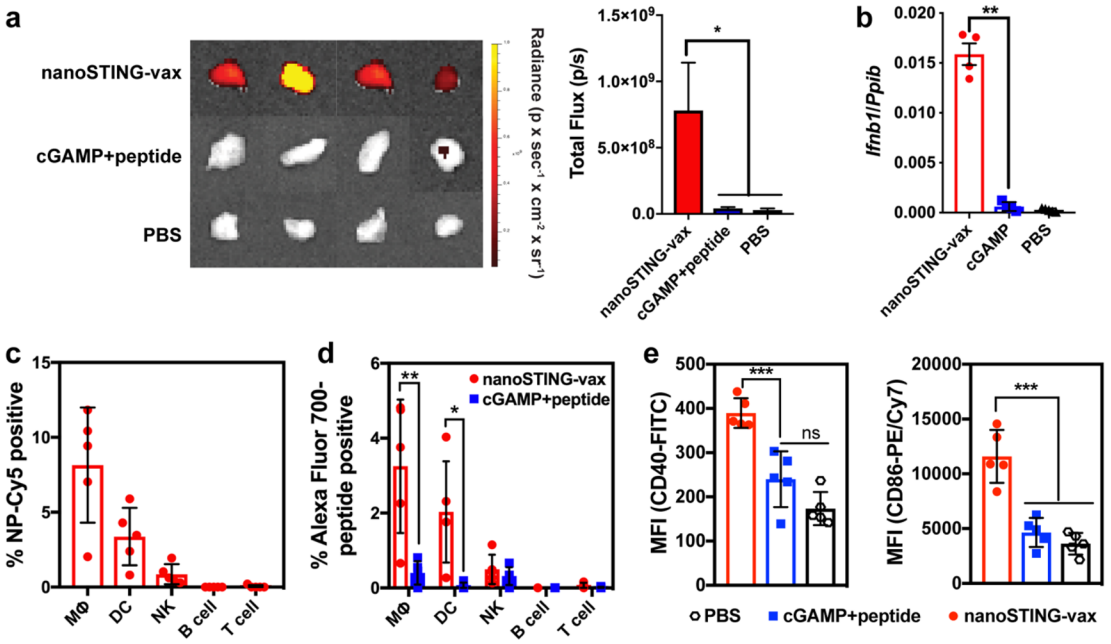

Figure 3. NanoSTING-vax improves delivery of cGAMP and peptide antigens to vaccine site draining LNs. (a) Representative images (left) and IVIS quantification of fluorescence (right) of the vaccine site draining inguinal LN 18 h following subcutaneous administration of nanoSTING-vax containing an Alexa Fluor 700-labeled peptide or a soluble mixture of Alexa Fluor 700-peptide and cGAMP (mean ± SEM; n = 8−10 mice/group; *P < 0.05; one-way ANOVA with Tukey posthoc test). (b) *Ifnb1* expression in the inguinal LN 4 h following administration of indicated vaccine formulation (mean ± SEM; n = 4−5 mice/group; ****P < 0.001; one-way ANOVA with Tukey posthoc test). (c) Percentage of NP-Cy5$^+$ cells among cell populations in the inguinal LN following administration of the labeled nanoparticle (n = 5 mice/group). MΦ, macrophage; DC, dendritic cell; NK, natural killer cell. (d) Percentage of Alexa Fluor 700-peptide$^+$ cells among cell populations in the inguinal LN following administration of the indicated formulation (n = 5 mice/group; two-tailed Student's t-test; *P < 0.05, **P < 0.01). MΦ, macrophage; DC, dendritic cell; NK, natural killer cell. (e) Flow cytometric quantification (MFI) of CD86 and CD40 expression by CD11c$^+$ DCs in the inguinal LN in response to immunization with the indicated formulation (n = 5 mice/group; ***P < 0.001, ****P < 0.0001; one-way ANOVA with Tukey posthoc test).

We next investigated the effect of co-delivery of peptide antigen and cGAMP on MHC-I antigen presentation using a model synthetic long peptide containing the immunodominant CD8$^+$ T cell epitope from ovalbumin (Ova), SIINFEKL. We first evaluated the SIINFEKL-specific CD8$^+$ T cell response in a co-culture assay comprising DC2.4 DCs and a B3Z CD8$^+$ T cell hybridoma that produces β-galactosidase upon recognition of SIINFEKL in complex with the H-2K^b molecule (Figure 2d). Co-delivery of antigen and cGAMP in polymersomes (*i.e.*, nanoSTING-vax) enhanced B3Z T cell activation to a greater extent than nanoparticles loaded only with peptide (NP-peptide), free peptide, or a mixture of soluble cGAMP and peptide. This is consistent with the ability of endosomolytic materials to promote cytosolic delivery of antigen, which enhances presentation on MHC-I,[53,54] a process that was further augmented *via* induction of STING signaling. Similar results were observed in bone marrow derived DCs (BMDCs) using an antibody against the H-2K^b/SIINFEKL complex (Figure 2e). Interestingly, in these studies, a mixture of free peptide and nanoparticles loaded only with cGAMP (NP-cGAMP + peptide) enhanced SIINFEKL presentation to a similar extent as nanoSTING-vax. This may reflect the capacity of STING signaling and IFN-I to promote antigen cross-presentation and increase surface expression of MHC-I[48,56,57] and/or a spontaneous physical association between the peptide and polymersomes postassembly that resulted in enhanced intracellular uptake and antigen presentation. Consistent with their capacity to enhance cGAMP activity, we also found that all polymersomes loaded with cGAMP (*i.e.*, nanoSTING-vax and NP-cGAMP) increased expression of the DC maturation marker MHC-II and the co-stimulatory molecules CD40 and CD86 to a greater extent than free cGAMP or nanoparticle formulations lacking cGAMP (Figure 2f), reflecting the relatively weak intrinsic adjuvant activity of the nanoparticle and the need for co-delivery of cGAMP. Collectively, these data demonstrate the capacity of endosomolytic polymersomes to mediate cytosolic dual-delivery of CDN STING agonists and peptide antigens, resulting in coordinated DC activation and antigen presentation, which, in turn, enhances CD8$^+$ T cell activation.

An attractive feature of nanoparticle vaccines is their ability to promote the biodistribution of vaccine components to LNs, with attendant enhancement in antigen presentation, APC maturation, and T cell priming.[55,58] To evaluate the distribution of vaccine components to the LN *in vivo*, vaccine formulations containing fluorescently labeled polymersomes (Cy5-labeled) and peptide (Alexa Fluor 700-labeled SGLEQ-LESIINFEKL) were administered subcutaneously to allow for monitoring of carrier and cargo distribution to a vaccine site draining LN (inguinal) and uptake by leukocytes in the LN. Fluorescent imaging of inguinal LNs isolated 18 h following injection demonstrated that loading of peptide antigen into polymersomes significantly increased antigen accumulation in the LN (Figure 3a). Additionally, a significant increase in the expression of *Ifnb1* in the inguinal LN was observed 4 h after administration (Figure 3b), demonstrating the ability of nanoSTING-vax to enhance cGAMP delivery to vaccine site draining LNs. Flow cytometric analysis of LNs 24 h post-

https://dx.doi.org/10.1021/acsnano.0c02765
ACS Nano 2020, 14, 9904−9916

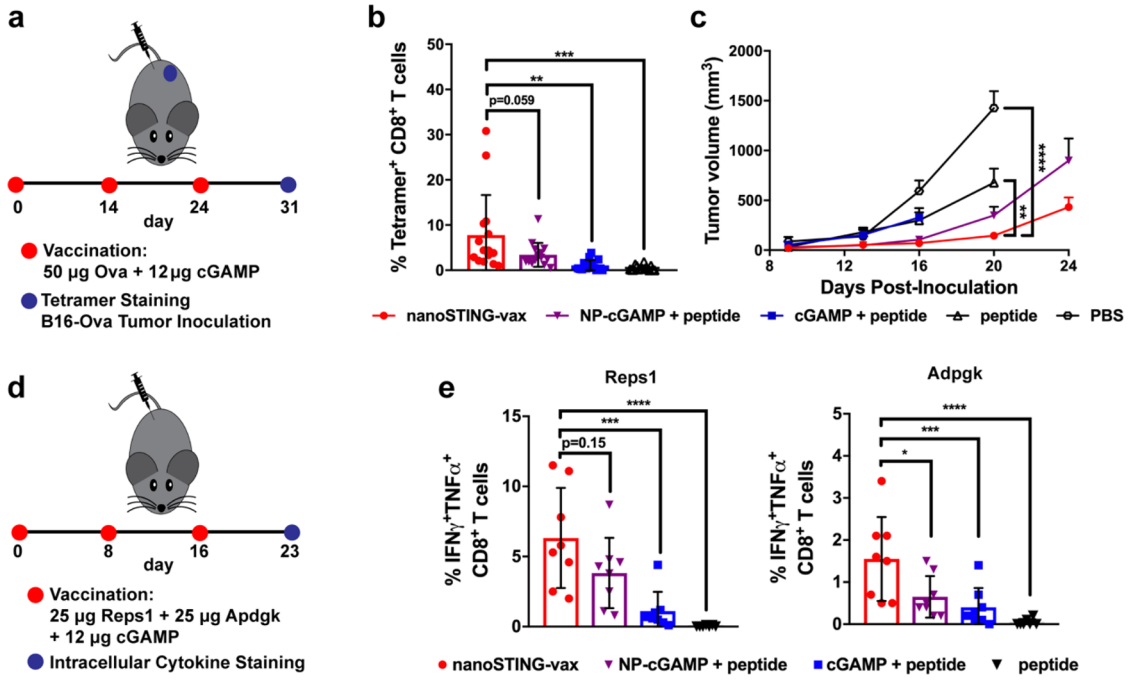

Figure 4. NanoSTING-vax enhances CD8$^+$ T cell responses to peptide antigens. (a) Administration, analysis, and tumor challenge scheme for mice immunized with nanoSTING-vax or indicated control formulations containing Ova peptide. (b) Quantification of the frequency of SIINFEKL-specific CD8$^+$ T cells in peripheral blood *via* peptide/MHC tetramer staining (n = 15 mice/group. Statistical significance between nanoSTING-vax and all other formulations are shown; ***P < 0.001, ****P < 0.0001; one-way ANOVA with Tukey posthoc test). (c) Average tumor volume following challenge of mice immunized with indicated vaccine formulations with B16-Ova cells (n = 8−15; mice/group; **P < 0.01, ****P < 0.0001; one-way ANOVA with Tukey posthoc test on day 20). (d) Administration scheme for mice immunized with nanoSTING-vax containing Reps1 and Adpgk neoantigenic peptides or indicated control formulations. (e) Percentage of IFN-γ^+TNF-α^+CD8α^+ T cells in peripheral blood after *ex vivo* restimulation with Reps1 and Adpgk epitopes and intracellular cytokine staining followed by flow cytometric analysis (n = 7−8 mice/group; *P < 0.05, ***P < 0.001, ****P < 0.0001; one-way ANOVA with Tukey posthoc test). Statistical data are presented as mean ± SD unless otherwise indicated.

immunization revealed that both peptide and polymer accumulated primarily in CD11b$^+$F4/80$^+$ macrophages and CD11c$^+$ DCs (Figure 3c,d; Figure S4b), which play direct roles in antigen presentation to T cells; minimal uptake of peptide or polymer was observed in NK cells, B cells, or T cells. Consistent with the data from *in vitro* experiments, nanoSTING-vax also resulted in increased expression of CD80 and CD86 co-stimulatory molecules on CD11c$^+$ DCs in the LN (Figure 3e; Figure S4c). Collectively, these data demonstrate the ability of the nanoSTING-vax platform to enhance peptide antigen and CDN delivery to APCs residing in draining LNs, a critical process in stimulation of cellular adaptive immunity.

We next evaluated the capacity of nanoSTING-vax to enhance CD8$^+$ T cell responses *in vivo* using a synthetic long peptide (SGLEQLESIINFEKL) containing the H-2K^b-restricted Ova epitope, SIINFEKL. Mice were administered the nanoSTING-vax, a soluble mixture of peptide and cGAMP, peptide only, or PBS (vehicle) and boosted on day 14 and 24 (Figure 4a). Additionally, based on the data from *in vitro* experiments demonstrating that mixing soluble peptide with cGAMP-loaded NPs (NP-cGAMP + peptide) could enhance antigen presentation, we also included this formulation as an additional control in these studies. On day 31, peptide/MHC-I tetramer staining was used to evaluate the magnitude of the SIINFEKL-specific CD8$^+$ T cell response in peripheral blood. NanoSTING-vax generated the highest antigen-specific CD8$^+$ T cell response of all of formulations tested, resulting in ∼8% SIINFEKL-specific CD8$^+$ T cells in the blood, whereas free peptide and a soluble mixture of cGAMP and peptide elicited responses undetectable from baseline (Figure 4b). Similar to *in vitro* findings, a slight, but statistically insignificant, increase in the percentage of tetramer-positive CD8$^+$T cells was observed for free peptide mixed with cGAMP-loaded NPs. As a functional validation of the CD8$^+$ T cell response, we challenged immunized mice on day 32 with a subcutaneous inoculation of Ova-expressing B16.F10 murine melanoma cells (B16-Ova) and evaluated tumor growth. Consistent with tetramer staining, only immunization with nanoSTING-vax resulted in significant inhibition of tumor growth (Figure 4c). Collectively, these experiments demonstrate that co-delivery of cGAMP and synthetic long peptides with endosomolytic polymersomes can significantly enhance the immunogenicity of peptide vaccines.

We next evaluated the capacity of nanoSTING-vax to enhance CD8$^+$ T cell responses to two established tumor neoantigenic peptides arising from mutations in the proteins Reps1 (AQLANDVVL) and Adpgk (ASMTNMELM) in the MC38 murine colon adenocarcinoma cell line.[59] In these studies, polymersomes were co-loaded with cGAMP and a synthetic long peptides containing either the Reps1 or Adpgk neoepitope, and the two formulations were then mixed to generate a vaccine containing both neoantigenic targets at equal peptide doses, as was done in recent clinical trials of multiepitope cancer vaccines.[60] First, nontumor bearing mice were immunized with nanoSTING-vax or indicated control formulations and boosted on days 8 and 16 (Figure 4d). The magnitude and functionality of the neoantigen-specific T cell response was evaluated *via* peptide restimulation of peripheral

https://dx.doi.org/10.1021/acsnano.0c02765
ACS Nano 2020, 14, 9904−9916

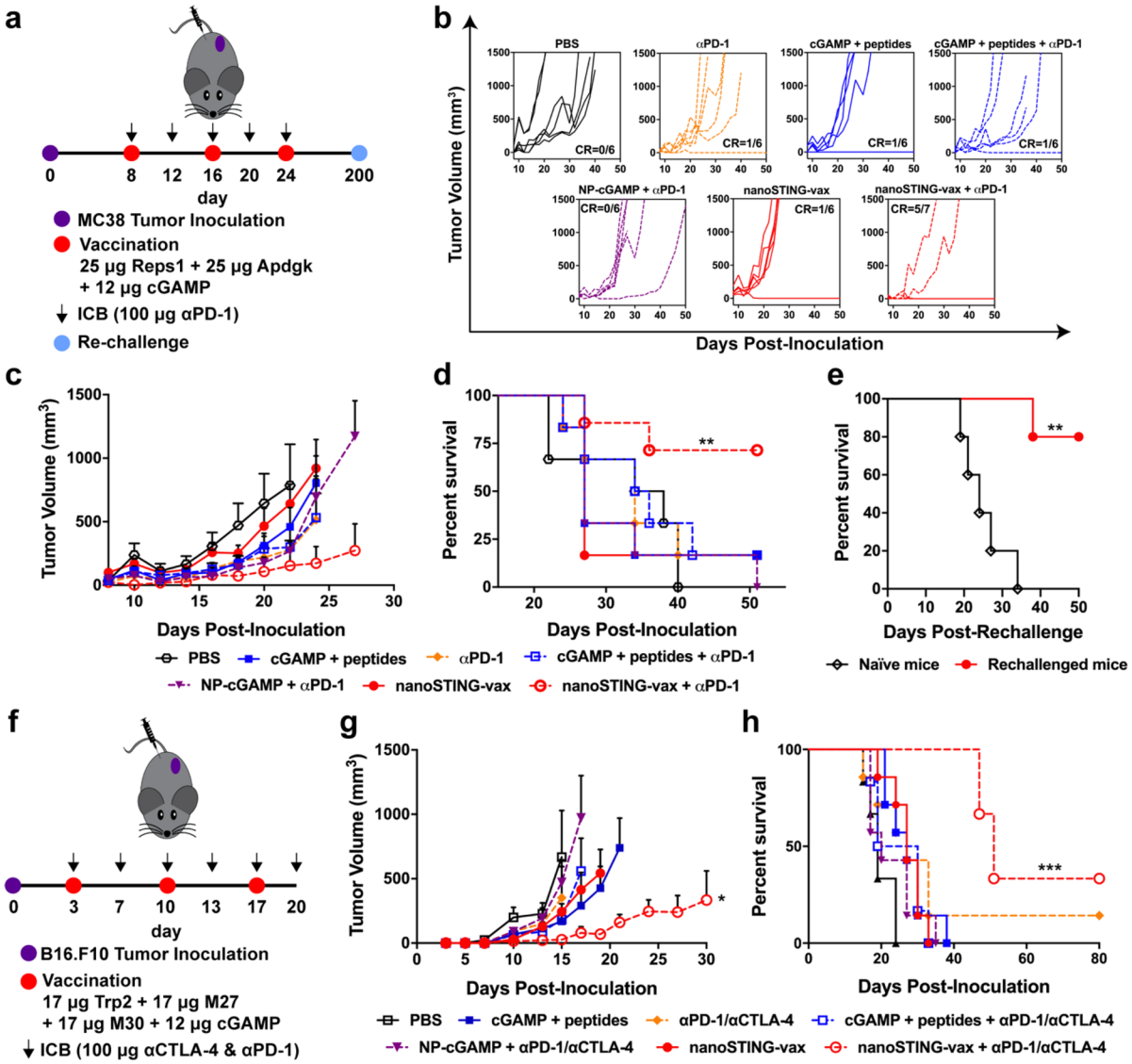

Figure 5. NanoSTING-vax enhances response to immune checkpoint blockade. (a) Tumor inoculation, therapeutic vaccination, immune checkpoint blockade regimen, and rechallenge scheme for mice with subcutaneous MC38 tumors. (b) Spider plots of individual tumor growth curves, with the numbers of complete responders denoted. (c) Average MC38 tumor volume in response to indicated treatment (n = 6−7 mice/group; $^*P < 0.05$; unpaired t test of nanoSTING-vax + αPD-1 *vs* NP-cGAMP + αPD-1 on day 27). (d) Kaplan−Meier survival curves of mice growing MC38 tumors treated with the indicated formulation using a 1500 mm^3 tumor volume as the end point criteria (n = 6−7 mice/group; $^{**}P < 0.01$; two-tailed Mantel−Cox test). (e) Kaplan−Meier survival curves for treatment naïve and mice demonstrating complete responses to nanoSTING-vax + αPD-1 after challenge with MC38 cells on the contralateral flank after 200 d without any further treatment (n = 5 mice; $^{**}P < 0.01$; two-tailed Mantel−Cox test). (f) Tumor inoculation, therapeutic vaccination, immune checkpoint blockade regimen for mice with subcutaneous B16.F10 tumors. (g) Average B16.F10 tumor volume in response to indicated treatment (n = 6−7 mice/group; $^*P < 0.05$; unpaired t test of nanoSTING-vax + αPD-1 + αCTLA-4. cGAMP + peptides on day 21). (h) Kaplan−Meier survival curves of mice growing B16.F10 tumors treated with the indicated formulation using a 1500 mm^3 tumor volume as the end point criteria (n = 6−7 mice/group; $^{***}P < 0.001$; two-tailed Mantel−Cox test). All statistical data are presented as mean ± SEM.

blood mononuclear cells (PBMCs) followed by intracellular cytokine staining for IFNγ and TNFα. Consistent with findings using SIINFEKL as a model antigen, nanoSTING-vax enhanced the frequency of polyfunctional (IFNγ^+TNFα^+) antigen-specific CD8$^+$ T cells relative to a mixture of synthetic long peptide and free cGAMP (Figure 4e). Interestingly, a mixture of free peptide and cGAMP-loaded NPs (NP-cGAMP + peptide) resulted in a statistically significant increase in the percentage of IFNγ^+TNFα^+ CD8$^+$ T cells for the Adpgk antigen, but not for Reps1, potentially reflecting a differential capacity of different peptides to spontaneously associate with polymersomes postassembly. To further investigate this, we used size exclusion chromatography to evaluate the extent to which the peptides employed in this study spontaneously associated with preformed polymersomes (Figure S5). While variable levels of interaction were observed, SGLEQLESIINFEKL and Reps1 displayed the highest level of association, whereas the Adpgk peptide interacted only minimally. While the stability or nature of such interactions remains to be elucidated, such data demonstrating that a mixture of free peptide and nanoparticles loaded with cGAMP (NP-cGAMP + peptide) can enhance immune responses to some synthetic long peptides highlight a potential opportunity to design peptide antigens that can spontaneously and efficiently

https://dx.doi.org/10.1021/acsnano.0c02765
ACS Nano 2020, 14, 9904−9916

integrate with preassembled cGAMP-loaded NPs. Designing peptides that enable such a "mix-and-go" nanoSTING-vax formulation merits future investigation as a strategy to further streamline the just-in-time manufacturing of personalized cancer vaccine products.[9,20,54] Nonetheless, these studies validate the ability of the nanoSTING-vax platform to enhance $CD8^+$ T cell responses to multiple neoantigenic peptides.

Based on the capacity of nanoSTING-vax to enhance neoantigen-specific $CD8^+$ T cell responses, we next evaluated whether this could be leveraged to improve responses to immune checkpoint blockade in a therapeutic vaccine setting. Many cancers can evade immune recognition through the expression of PD-L1 in response to secretion of IFN-γ by infiltrating T cells, resulting in inhibition of cytotoxic T cell function *via* binding to PD-1 on T cells.[2] Therefore, maximizing the efficacy of cancer vaccines often requires a blockade of PD-1, PD-L1, or other immune checkpoint molecules (*e.g.*, CTLA-4) to circumvent this resistance mechanism.[10] We first used the MC38 murine colorectal adenocarcinoma model, which has known neoantigens and expresses PD-L1, but is largely resistant to PD-L1/PD-1 blockade owing to a highly immunosuppressive microenvironment.[61] Mice were inoculated subcutaneously with MC38 cells and vaccinated starting on day 8 with nanoSTING-vax or control formulations (Figure 5a). Additionally, nanoSTING-vax and selected controls were combined with systemic (i.p.) administration of anti-PD-1 antibody (αPD-1) which has minimal therapeutic effect when delivered as monotherapy. While the nanoSTING-vax conferred minimal therapeutic benefits alone in this model, we observed a dramatic improvement in the response to αPD-1, resulting in a ~70% (5/7 mice) complete response rate, as indicated by the absence of any outward evidence of tumor growth up to 200 days postvaccination (Figure 5b–d). Importantly, eliminating peptide antigens from the vaccine formulation (NP-cGAMP + αPD-1) nearly entirely abrogated therapeutic benefit, indicating that a vaccine-induced, antigen-specific T cell response was critical to the efficacy observed. To evaluate the capacity of nanoSTING-vax in combination with αPD-1 to generate immunological memory with potential to prevent disease recurrence, we rechallenged complete responders ~180 days following the last vaccine treatment. Several months after cessation of treatment and in mice of a more advanced age (~36 weeks), the combination of nanoSTING-vax and αPD-1 resulted in significant protection from tumor rechallenge, with 4/5 mice remaining tumor free for at least 30 days (Figure 5e).

While including peptide neoantigens into the formulation was critical to achieving complete responses and long-term survival, it was notable that a slight, but statistically significant ($P < 0.01$), decrease in tumor volume was observed in the nanoSTING-vax + αPD-1 group compared to PBS on day 10, only 2 days after initial vaccination and too early for such effects to be mediated by vaccine-induced T cells. We have previously demonstrated that intravenous administration of NP-cGAMP could inhibit tumor growth and improve response to immune checkpoint blockade,[38] and it has also been shown that peripherally administered nanoparticles can access the circulation *via* lymphatic drainage.[62] We therefore investigated the possibility that subcutaneous vaccination with nanoSTING-vax may induce systemic STING activation. Mice were administered NP-cGAMP subcutaneously and serum levels of several established STING-driven cytokines (IFN-α, TNFα, IL-6) were measured (Figure S6). We found that peripheral administration of NP-cGAMP resulted in a rapid and transient elevation of serum cytokines, consistent with systemic nanoparticle distribution. Therefore, it is possible that the observed tumor suppression at early time points, while modest, may result from a subset of nanoparticles that distribute systemically and exert direct effects on the tumor. This may be important for controlling tumor burden during priming and expansion of neoantigen-specific T cells as well as for inhibiting immunosuppression in the tumor microenvironment, both of which would be anticipated to enhance the efficacy of T cells elicited *via* vaccination.[7] A similar concept was demonstrated by Zhang *et al.*, who intravenously administered immunostimulatory nanoparticles to reduce tumor burden and inhibit immunosuppression to improve the ability of CAR T cells to infiltrate solid tumors.[63] The possibility that nanoSTING-vax may act both *via* generation of neoantigen-specific T cells and by mediating direct effects on the tumor microenvironment that enhance vaccine efficacy merits future exploration. Additionally, while we have previously demonstrated that intravenous administration of NP-cGAMP is well-tolerated,[38] the stimulation of a systemic cytokine response nonetheless raises important questions regarding toxicity and safety that will need to be addressed. It is notable that an mRNA-based cancer vaccine that was administered intravenously in humans also induced a similar type of systemic cytokine response, with patients experiencing only transient flu-like symptoms.[64] Nonetheless, additional research is necessary to optimize nanoSTING-vax dose, to modulate the extent of systemic distribution, and to further understand and manage potential toxicities.

Finally, we evaluated the nanoSTING-vax platform in an aggressive and poorly immunogenic B16.F10 melanoma model, which is highly resistant to immune checkpoint inhibitors and is difficult to treat using conventional cancer vaccines.[19] Again, we utilized a mixture of nanoparticles, each loaded with a synthetic long peptide containing an established B16.F10 T cell epitope. Here, we used two neoantigens, the MHC class I epitope M27 and the MHC-II antigen M30, as well as the MHC-I restricted epitope $Trp2_{180–188}$ from the melanoma-associated antigen tyrosinase-related protein 2 (TRP2).[19,65] This strategy of combining shared tumor-associated antigens (*e.g.*, TRP2) with individualized neoantigens has recently been explored in a clinical trial for glioblastoma.[66] Mice were vaccinated with nanoSTING-vax comprising a pool of all three peptides at an equal dose (Figure 5f). Similar to our results in the MC38 model, vaccination with nanoSTING-vax alone did not confer significant therapeutic benefits, likely a consequence of the highly immunosuppressive microenvironment that is rapidly established in these tumor models.[61] Nonetheless, nanoSTING-vax in combination with αPD-1 + αCTLA-4, the most aggressive immune checkpoint inhibitor regimen used clinically, significantly inhibited tumor growth and extended mean survival time, leading to complete rejection in ~30% (2/6) of treated mice (Figure 5g,h). As in the MC38 model, minimal tumor suppression was observed in all other groups, including an analogous vaccine formulation lacking peptide antigens, further indicating that the induced antigen-specific T cell response is critical to enhancing responses to immune checkpoint blockade.

CONCLUSION

Immune checkpoint blockade continues to expand the treatment of diverse cancer types. Nonetheless, a growing

https://dx.doi.org/10.1021/acsnano.0c02765
ACS Nano 2020, 14, 9904–9916

body of clinical evidence has demonstrated that complete and durable responses to immune checkpoint inhibitors are still the exception rather than the rule. This disappointing outcome is largely attributed to an insufficient antitumor T cell response that can be reinvigorated by immune checkpoint inhibitors, fueling the clinical exploration of neoantigen vaccines targeting patients' tumor-specific mutations. Inspired by endogenous mechanisms of tumor immune surveillance, here we describe a platform for personalized cancer vaccines, nanoSTING-vax. NanoSTING-vax elicits robust antigen-specific $CD8^+$ T cell responses *via* a dual-delivery of peptide antigens and CDN STING agonists to the cytosol. Owing to its nanoscale properties, the ability to enhance antigen cross-presentation, and potent immunostimulatory capacity, nanoSTING-vax is an enabling technology for increasing the immunogenicity of peptide antigens, resulting in the generation of antigen-specific T cell responses capable of rejecting pre-established, poorly immunogenic tumors when administered in combination with immune checkpoint blockade antibodies. Furthermore, nanoSTING-vax enables co-loading of CDNs and a wide range of peptide antigens of variable length and composition, offering a versatile vaccine delivery system that is well-suited for integration into current neoantigen vaccine production pipelines. Additionally, due to their vesicular structure, polymersomes are amenable to loading molecules of diverse physiochemical properties and, hence, may also provide a versatile template for coordinating the delivery of adjuvant combinations that can act in synergy with CDNs[67−69] to augment or shape cellular immunity to personalized cancer vaccines. In summary, nanoSTING-vax—endosomolytic nanoparticles designed for dual-delivery of CDN STING agonists and peptide antigens—is a promising platform for improving responses to personalized cancer vaccines, particularly in combination with immune checkpoint inhibitors.

MATERIALS AND METHODS

NanoSTING-vax Fabrication. Poly[(ethylene glycol)-*block*-[(2-diethylaminoethyl methacrylate)-*co*-(butyl methacrylate)-*co*-(pyridyl disulfide ethyl methacrylate)]] (PEG-DBP) was synthesized and characterized as previously described and detailed in the Supporting Information.[38] A phosphorothioated cGAMP analog (RpRp dithio 2′3′cGAMP) was synthesized using a method adapted from Gaffney *et al.* and described in detail in the Supporting Information.[70] Synthetic long peptides containing established epitopes were purchased from Elim Biopharmaceuticals. Synthetic long peptides used in this study include: Ova (SGLEQLESIINFEKL), Reps1 (RVLELFRAAQLANDDVVLQIMELC), Adpgk (GIPVHLELASMTNMELMSSIVHQQVF), TRP2 (SVYDFFVWL), M27 (REGVELCPGNKYEMRRHGTTHSLVIHD), and M30 (PSKPSFQEFVDWENVSPELNSTDQPFL). NanoSTING-vax was formulated using polymersome self-assembly methods as previously described[38] with a minor modification to allow for cGAMP and peptide coencapsulation. PEG-DBP was dissolved in a small quantity of ethanol to a concentration of 1250 mg/mL, followed by addition of a solution of 25 mg/mL OF cGAMP in DI H_2O and 50 mg/mL of water-soluble peptides (Ova) to drive polymer phase separation and cargo encapsulation. Less water-soluble peptides (Reps1, Adpgk, M27, M30, TRP2) were dissolved in DMSO (50 mg/mL) and directly incorporated into the organic ethanolic phase prior to addition of the aqueous cGAMP solution. The volume of cGAMP added to the polymer solution was varied based on the average encapsulation efficiency of each peptide to ensure all formulations had the same peptide to cGAMP mass ratio of 4:1. Gradual dilution into DI H_2O with sonication dispersed the polymer gel into colloidally stable nanoparticles, whereupon the formulation was cross-linked *via* addition of 0.5 equiv of dithiothreitol (DTT) relative to PDSMA groups. Unencapsulated cargo was removed *via* ultracentrifugal filtration through a 50,000 MWCO membrane to yield nanoSTING-vax nanoparticles. Control particles were formulated *via* the exact same method by simply omitting the addition of either the cGAMP or peptide solution. To quantify cGAMP and peptide loading, an aliquot was removed and diluted in pH 5.8 PBS to disassemble the vesicles and then analyzed by high-performance liquid chromatography with a gradient mobile phase from 0.1% trifluoroacetic acid (TFA) in water to 0.1% TFA in acetonitrile over 10 min. cGAMP concentration was measured at 260 nm, and peptide concentration was measured at 214 nm. Nanoparticle size distribution and ζ potential were measured by diluting particles in PBS (pH 7.4) and characterized using a Malvern Nano ZS. For transmission electron microscopy, particles were drop cast onto carbon Type-B support grid (Ted Pella), stained with NANO-W negative stain (Nanoprobes), and imaged on a 200 kV Osiris transmission electron microscope in high-contrast mode with a 20 μm objective aperture.

Analysis of Spontaneous Association of Peptides with Nanoparticle. In order to measure the ability of each peptide to spontaneously associate with the preformulated polymersomes, each peptide was mixed with the polymersomes and then run down a Sephadex G-50 column equilibrated with PBS. The polymersomes were collected, and any peptide that co-eluted with the polymersomes was measured using fluoraldehyde *o*-phthaldiadlehyde reagent solution. Separately, the same volume and quantity of peptide alone was run down the column, the same fraction was collected, and the amount of peptide was again quantified. The amount of peptide in this control was subtracted from the amount of peptide associated with the polymersome, and the percent associated peptide was calculated.

***In Vitro* Evaluation of cGAMP Activity.** cGAMP activity was measured using RAW-Blue ISG cells (InvivoGen) that were cultured in DMEM supplemented with 10% FBS, 4.5 g/L of glucose, 2 mM L-glutamine, and 100 μg/mL of normacin. Zeocin (200 μg/mL) was added every other passage to maintain selection pressure. RAW-Blue ISG cells were seeded at a density of 50,000 cells/well in a 96-well plate and then treated with the indicated formulations and concentrations for 24 h. Relative expression of IFN-I was measured using QUANTI-Blue reagent (InvivoGen).

Evaluation of Dendritic Cell Antigen Presentation, Activation, and Cross-Priming. Bone marrow cells were harvested from the tibias of female C57BL/6J mice by flushing them with PBS and passing the cell suspension through a 70 μm cell strainer. Cells were then cultured on noncell culture treated plates in RPMI 1640 medium supplemented with 2 mM L-glutamine, 10% heat inactivated FBS, 0.4 mM sodium pyruvate, 50 μM β-mercaptoethanol, and 20 ng/mL of GM-CSF to induce differentiation into BMDCs. Fresh media was added on days 4 and 7, and on day 8, cells were replated in 12-well plates at 10^5 cells per well. Cells were then treated with vaccine formulations containing 500 nM SGLEQLESIINFEKL peptide and/or 100 ng/mL of cGAMP for 24 h. Following incubation, cells were scraped, washed with cold PBS, and stained with antibodies against SIINFEKL/H-$2K^b$ and markers of DC activation (MHC-II, CD40, CD86) followed by flow cytometric analysis (Amnis CellStream, Luminex). The following antibodies were used for these studies: αCD40: (30-F11, FITC, BioLegend), αCD86 (GL-1, PE/Cy7, BioLegend), $\alpha Ova_{257-264}$-H-$2K^b$ (PE, eBioscience), and αI-A/I-E (M5/114.15.2, APC/Cy7, BioLegend).

To evaluate cross-priming of T cells, a co-culture model comprising DC2.4 dendritic cells and a B3Z T cell hybridoma that produces β-galactosidase upon recognition of SIINFEKL/H-$2K^b$ was used.[71] The mouse DC line DC2.4 (H-$2K^b$-positive) was kindly provided by K. Rock (University of Massachusetts Medical School), and B3Z T cells were a generous gift from Nilabh Shastri (UC Berkeley). DC2.4 cells were cultured in RPMI 1640 media supplemented with 10% FBS, 1% penicillin and streptomycin, 2 mM L-glutamine, 10 mM HEPES, 1 × nonessential amino acids, and 55 μM β-mercaptoethanol in 96-well plates at a density of 10,000 cells/well. Cells were treated with vaccine formulations in a working concentration of 500 nM SGLEQLESIINFEKL peptide and/or 100 ng/mL cGAMP for 24 h. Following

https://dx.doi.org/10.1021/acsnano.0c02765
ACS Nano 2020, 14, 9904−9916

incubation, media was aspirated, and 10^5 B3Z cells in RPMI 1640 supplemented with 10% FBS, 100 U/mL penicillin/100 μg/mL streptomycin, 50 μM 2-mercaptoethanol, and 1 mM sodium pyruvate were added to cell culture wells and cultured for 24 h. Cells were then pelleted, and media were aspirated and replaced with lysis buffer consisting of 0.1% Triton, 0.15 mM chlorophenol red-β-D-galactopyranoside (Sigma), 9 mM MgCl, and 100 μM β-mercaptoethanol. After incubation for 90 min at 37 °C, the magnitude of antigen recognition was evaluated through absorbance measurements (λ = 570 nm).

***In Vivo* Analysis of Lymph Node Accumulation, Cellular Uptake, and Dendritic Cell Activation.** Female C57BL/6J mice (6–8 weeks old) were purchased from The Jackson Laboratory (Bar Harbor, ME) and maintained at the animal facilities of Vanderbilt University Medical Center under conventional conditions. All animal experiments were approved by the Vanderbilt University Institutional Animal Care and Use Committee (IACUC). To evaluate LN accumulation and cellular uptake, C57BL/6J mice were injected subcutaneously at the base of tail with formulations containing Alexa Fluor 700-labeled SGLEQLESIINFEKL (Elim Biopharmaceuticals) and Cy5-labeled polymersomes, which were generated by incorporating Cy5-labeled PEG-DBP that was synthesized *via* partial reduction of PDSMA groups followed by reaction with Cy5-maleimide (Abcam). After 18 h, inguinal LNs were harvested, and the Alexa Fluor 700 fluorescence signal was measured with IVIS optical imaging system (Caliper Life Sciences). Following imaging of the LN, single cell suspensions were prepared and stained with a panel of the antibodies BV650-αCD45 (30-F11), PE/Cy5-αCD11b (M1/70), PE/Cy5-αCD11c (N418), PE-αNK1.1 (PK136), PE/Cy7-αF4/80 (BM8), PE/Cy7-αCD86 (GL-1), and BV510-αCD3 (17A2) (BioLegend). Cells were then washed and analyzed on a BD LSR Fortessa flow cytometer. Representative flow cytometry data and gating strategies for defining cell populations and determining cellular uptake are shown in Figure S4.

***Ifnb1* Expression in the Lymph Node.** C57BL/6J mice were injected subcutaneously at the base of tail with PBS, a mixture of peptide and cGAMP, or nanoSTING-vax. After 4 h, the inguinal LNs were harvested and placed in RLT lysis buffer (Qiagen) supplemented with 2% β-mercaptoethanol (Sigma) in a gentleMACS M tube with mechanical disruption using an OctoMACS tissue dissociator (Miltenyi). Tumor RNA was isolated with a RNeasy RNA isolation kit (Qiagen) with the RNase-free DNase Set (Qiagen), used according to manufacturer's specifications. Complementary DNA (cDNA) was synthesized with the Bio-Rad iScript cDNA kit and analyzed *via* qPCR using the appropriate TaqMan kits (Thermo Fisher Scientific). The TaqMan gene expression kits were: Mm00439552_s1 for mouse *Ifnb1* and Mm00478295-m1 for mouse *Ppib*.

***In Vivo* Immunization and Analysis of T Cell Response.** To evaluate the $CD8^+$ T cell response elicited by formulations containing SGLEQLESIINFEKL, mice (6–8 week) were immunized *via* subcutaneous injection at the base of the tail on days 0, 14, and 24 with formulations containing 50 μg of peptide and 12 μg of cGAMP in PBS. At day 31, whole blood was treated with ACK lysis buffer (Gibco), washed, resuspended in cold PBS supplemented with 2% FBS and 50 μM dasatinib, and stained with PE-labeled peptide-MHC tetramer (H-$2K^b$-restricted SIINFEKL, NIH Tetramer Core Facility, Atlanta, GA) and the following antibodies: αCD45(30-F11, PE/Cy5, BioLegend), αCD3 (17A2, APC, BioLegend), and αCD8 (KT15, FITC, ThermoFisher). After 1 h, cells were washed with PBS supplemented with 2% FBS and 50 μM dasatinib and stained with propidium iodide (BD Biosciences) to discriminate live from dead cells. Flow cytometry (BD LSRII) was used to determine the frequency of SIINFEKL-specific $CD8^+$ T cells. Representative flow cytometry data and gating strategies for determining the frequency of $tetramer^+CD8^+$ T cells are shown in Figure S6.

To evaluate responses to vaccines containing Reps1 and Adpgk, mice were immunized on days 0, 8, and 16 *via* subcutaneous injection at the base of the tail. In all studies where multiple peptides were used, independent nanoSTING-vax preparations were prepared for each peptide and then pooled prior to administration. On day 23, blood was harvested, treated with ACK lysis buffer, and plated at a density of 2×10^6 cells per well in 12-well plates in RPMI 1640 supplemented with 10% FBS. Cells were treated for 6 h with exact peptides for mutant Reps1 (AQLANDVVL) or Adpgk (ASMTNMELM) at a concentration of 10 μg/mL for 6 h. At the second hour, media was supplemented with brefeldin A (Biolegend) according to manufacturer specifications. Following incubation, cells were harvested and stained with αCD3 (17A2, APC, BioLegend), αCD8a (53.6.7, PE/Cy5, BioLegend) and αCD4 (RM4–5, APC/Cy7, BioLegend). Cells were then washed and fixed using fixation buffer (BioLegend), permeabilized with intracellular staining permeabilization wash buffer (BioLegend), and stained with αIFNγ (XMG1.2, Alexafluor488, BioLegend) and αTNFα (MP6-XT22, PE, BioLegend) before flow cytometric quantification of the percentage of $TNF\alpha^+$ and $IFN\gamma^+$ $CD8^+$ T cells (BD LSR II). Representative flow cytometry data and gating strategies for determining the frequency of $TNF\alpha^+$ and $IFN\gamma^+$ $CD8^+$ T cells are shown in Figure S7.

Tumor Studies. For the prophylactic tumor challenge studies, mice vaccinated with formulations containing 50 μg of SGLEQLESIINFEKL, as described above, were challenged 7 days following the final vaccination by subcutaneous flank injection of 5×10^5 B16-Ova cells, generously provided by Amanda Lund (Oregon Health Sciences University). Tumor volume was measured every other day *via* caliper measurements using the formula $V = L \times W \times H/2$. Mice were euthanized at a tumor burden end point of 1500 $mm.^3$ For the MC38 therapeutic model, mice were inoculated subcutaneously on the flank with 10^6 MC38 cells (generously provided by Daniel Beauchamp, Vanderbilt University) and vaccinated on days 8, 16, and 24 *via* subcutaneous injection at the base of the tail. Vaccines consisted of 12 μg cGAMP and 25 μg each of Reps1 and Adpgk synthetic long peptides. Mice were administered αPD-1 (Clone, BioXCell) on days 8, 12, 16, 20, and 24 intraperitoneally, and tumor growth was monitored as described above. For the B16.F10 therapeutic vaccination model, mice were inoculated *via* subcutaneous flank injection with 5×10^5 B16.F10 cells (generously provided by Ann Richmond, Vanderbilt University). Mice were then vaccinated as described above on days 3, 10, and 17, with formulations containing 17 μg of the TRP2, M27, and M30 neoantigen peptides and 12 μg of cGAMP. αCTLA-4 and αPD-1 antibodies (100 μg each) were administered intraperitoneally on days 7, 10, 13, 17, and 20. Tumor growth was monitored as indicated above.

Analysis of Serum Cytokines. C57BL/6J mice were injected subcutaneously at the base of the tail with either PBS or nanoSTING-vax. At various time points (6, 24, 48, 72 h), blood was collected and allowed to clot. Serum was analyzed for amounts of TNF-α, IFN-α, and IL-6 *via* the LEGENDplex Multi-Analyte Flow Assay Kit (BioLegend) following manufacturer's instructions for the assay using a V-bottom plate. A 1:4 dilution was used for 6 and 24 h time points, while a 1:2 dilution was used for 48 and 72 h time points. Data were collected on a CellStream Flow Cytometer (Luminex) equipped with 405, 488, 561, and 642 nm lasers and analyzed with LEGENDplex Data Analysis software v8.0 (VigeneTech).

ASSOCIATED CONTENT

Supporting Information

The Supporting Information is available free of charge at https://pubs.acs.org/doi/10.1021/acsnano.0c02765.

Supplementary methods detailing polymer and cGAMP synthesis and supplementary data describing nanoSTING-vax properties and activity with different peptide antigens; additional transmission electron microscopy images; analysis of peptide association with nanoparticles; flow cytometry gating strategies; serum cytokine analysis; and chemical characterization of cGAMP (PDF)

https://dx.doi.org/10.1021/acsnano.0c02765
ACS Nano 2020, 14, 9904–9916

AUTHOR INFORMATION

Corresponding Author

John T. Wilson − *Department of Chemical and Biomolecular Engineering, Department of Biomedical Engineering, and Vanderbilt Institute of Chemical Biology, Vanderbilt University, Nashville, Tennessee 37235, United States; Department of Pathology, Microbiology, and Immunology, Vanderbilt Institute for Infection, Immunology, and Inflammation, Vanderbilt Center for Immunobiology, and Vanderbilt-Ingram Cancer Center, Vanderbilt University Medical Center, Nashville, Tennessee 37232, United States; Department of Veterans Affairs, Tennessee Valley Healthcare System, Nashville, Tennessee 37212, United States;* orcid.org/0000-0002-9144-2634; Email: john.t.wilson@vanderbilt.edu

Authors

Daniel Shae − *Department of Chemical and Biomolecular Engineering, Vanderbilt University, Nashville, Tennessee 37235, United States*

Jessalyn J. Baljon − *Department of Biomedical Engineering, Vanderbilt University, Nashville, Tennessee 37235, United States*

Mohamed Wehbe − *Department of Chemical and Biomolecular Engineering, Vanderbilt University, Nashville, Tennessee 37235, United States*

Plamen P. Christov − *Vanderbilt Institute of Chemical Biology, Vanderbilt University, Nashville, Tennessee 37232, United States*

Kyle W. Becker − *Department of Chemical and Biomolecular Engineering, Vanderbilt University, Nashville, Tennessee 37235, United States;* orcid.org/0000-0003-1627-2724

Amrendra Kumar − *Department of Pathology, Microbiology, and Immunology, Vanderbilt University Medical Center, Nashville, Tennessee 37232, United States; Department of Veterans Affairs, Tennessee Valley Healthcare System, Nashville, Tennessee 37212, United States*

Naveenchandra Suryadevara − *Department of Pathology, Microbiology, and Immunology, Vanderbilt University Medical Center, Nashville, Tennessee 37232, United States; Department of Veterans Affairs, Tennessee Valley Healthcare System, Nashville, Tennessee 37212, United States*

Carcia S. Carson − *Department of Biomedical Engineering, Vanderbilt University, Nashville, Tennessee 37235, United States*

Christian R. Palmer − *Department of Chemical and Biomolecular Engineering, Vanderbilt University, Nashville, Tennessee 37235, United States;* orcid.org/0000-0002-4184-0095

Frances C. Knight − *Department of Biomedical Engineering, Vanderbilt University, Nashville, Tennessee 37235, United States*

Sebastian Joyce − *Department of Pathology, Microbiology, and Immunology, Vanderbilt Institute for Infection, Immunology, and Inflammation, and Vanderbilt Center for Immunobiology, Vanderbilt University Medical Center, Nashville, Tennessee 37232, United States; Department of Veterans Affairs, Tennessee Valley Healthcare System, Nashville, Tennessee 37212, United States;* orcid.org/0000-0002-3183-1451

Complete contact information is available at: https://pubs.acs.org/10.1021/acsnano.0c02765

Author Contributions

◆These authors contributed equally to this work

Author Contributions

Conceptualization by D.S. and J.T.W.; methodology by D.S., S.J., and J.T.W.; investigation by D.S., J.J.B., M.W., P.C., K.W.B., A.K., N.S., C.S.C., C.P., and F.C.K.; resources from P.C., S.J., and J.T.W.; original draft writing by D.S. and J.T.W. and review and editing by D.S., J.J.B., S.J., and J.T.W.; visualization by D.S., J.J.B., and J.T.W.; supervision by J.T.W.; and funding acquisition by S.J. and J.T.W.

Notes

The authors declare the following competing financial interest(s): J.T.W. and D.S. are co-inventors on U.S. Patent Number 10,696,985 Reversibly Crosslinked Endosomolytic Polymer Vesicles for Cytosolic Drug Delivery.

ACKNOWLEDGMENTS

We gratefully acknowledge Kenneth Rock for providing DC2.4 cells, N. Shastri for providing B3Z T cells, A. Lund for providing B16-Ova cells, D. Beauchamp for providing MC38 cells, A. Richmond for providing B16.F10 cells, L. Glickman for consultation on peptide antigens, and C. Duvall for the use of gel permeation chromatography equipment and IVIS imaging system. We also thank Fairman Studios for illustrating the Table of Contents image and Figure 1. The following reagent was obtained through the NIH Tetramer Core Facility: PE-labeled SIINFEKL/H-2K^{b} tetramer. We thank the core facilities of the Vanderbilt Institute of Nanoscale Sciences and Engineering (VINSE) for use of dynamic light scattering and electron microscopy and the VUMC Flow Cytometry Shared Resource, supported by the Vanderbilt Ingram Cancer Center (P30 CA68485) and the Vanderbilt Digestive Disease Research Center (DK058404). 2′3′-cGAMP was provided by the Vanderbilt Institute of Chemical Biology Chemical Synthesis Core. This research was supported by grants from the National Science Foundation CBET-1554623 (J.T.W.), a Vanderbilt Ingram Cancer Center (VICC) Ambassador Discovery Grant (J.T.W.), a VICC-Vanderbilt Center for Immunobiology Pilot Grant (J.T.W.), the National Institutes of Health (NIH) 5R21AI121626 (J.T.W.) and 5R01DE027749 (S.J.), the Vanderbilt University Discovery Grant Program (J.T.W, S.J.), a Veteran's Affairs Merit Award BX001444 (S.J.), and also supported by a Stand Up To Cancer Innovative Research Grant, grant number SU2C-AACR-IRG 20-17 (J.T.W.). Stand Up To Cancer (SU2C) is a program of the Entertainment Industry Foundation. Research grants are administered by the American Association for Cancer Research, the scientific partner of SU2C. M.W. acknowledges a postdoctoral fellowship from the Canadian Institutes of Health Research (CIHR). C.S.C. acknowledges a National Science Foundation Graduate Research Fellowship under grant numbers DGE-1445197 and DGE-1937963.

REFERENCES

(1) Ribas, A.; Wolchok, J. D. Cancer Immunotherapy Using Checkpoint Blockade. *Science* **2018**, *359*, 1350−1355.

(2) Sharma, P.; Allison, J. P. The Future of Immune Checkpoint Therapy. *Science* **2015**, *348*, 56−61.

(3) O'Donnell, J. S.; Teng, M. W. L.; Smyth, M. J. Cancer Immunoediting and Resistance to T Cell-Based Immunotherapy. *Nat. Rev. Clin. Oncol.* **2019**, *16*, 151−167.

(4) Binnewies, M.; Roberts, E. W.; Kersten, K.; Chan, V.; Fearon, D. F.; Merad, M.; Coussens, L. M.; Gabrilovich, D. I.; Ostrand-Rosenberg, S.; Hedrick, C. C.; Vonderheide, R. H.; Pittet, M. J.; Jain, R. K.; Zou, W.; Howcroft, T. K.; Woodhouse, E. C.; Weinberg, R. A.;

Krummel, M. F. Understanding the Tumor Immune Microenvironment (TIME) for Effective Therapy. *Nat. Med.* **2018**, *24*, 541−550.
(5) Chen, D. S.; Mellman, I. Elements of Cancer Immunity and the Cancer-Immune Set Point. *Nature* **2017**, *541*, 321−330.
(6) Fridman, W. H.; Zitvogel, L.; Sautes-Fridman, C.; Kroemer, G. The Immune Contexture in Cancer Prognosis and Treatment. *Nat. Rev. Clin. Oncol.* **2017**, *14*, 717−734.
(7) Shae, D.; Baljon, J. J.; Wehbe, M.; Becker, K. W.; Sheehy, T. L.; Wilson, J. T. At the Bench: Engineering the Next Generation of Cancer Vaccines. *J. Leukocyte Biol.* **2019**. DOI: 10.1002/JLB.5BT0119-016R
(8) Scheetz, L.; Park, K. S.; Li, Q.; Lowenstein, P. R.; Castro, M. G.; Schwendeman, A.; Moon, J. J. Engineering Patient-Specific Cancer Immunotherapies. *Nat. Biomed Eng.* **2019**, *3*, 768−782.
(9) Tureci, O.; Lower, M.; Schrors, B.; Lang, M.; Tadmor, A.; Sahin, U. Challenges towards the Realization of Individualized Cancer Vaccines. *Nat. Biomed Eng.* **2018**, *2*, 566−569.
(10) Ott, P. A.; Wu, C. J. Cancer Vaccines: Steering T Cells Down the Right Path to Eradicate Tumors. *Cancer Discovery* **2019**, *9*, 476−481.
(11) Romero, P.; Banchereau, J.; Bhardwaj, N.; Cockett, M.; Disis, M. L.; Dranoff, G.; Gilboa, E.; Hammond, S. A.; Hershberg, R.; Korman, A. J.; Kvistborg, P.; Melief, C.; Mellman, I.; Palucka, A. K.; Redchenko, I.; Robins, H.; Sallusto, F.; Schenkelberg, T.; Schoenberger, S.; Sosman, J.; et al. The Human Vaccines Project: A Roadmap for Cancer Vaccine Development. *Sci. Transl. Med.* **2016**, *8*, 334ps9.
(12) Schumacher, T. N.; Schreiber, R. D. Neoantigens in Cancer Immunotherapy. *Science* **2015**, *348*, 69−74.
(13) Melief, C. J. M.; van der Burg, S. H. Immunotherapy of Established (Pre)Malignant Disease by Synthetic Long Peptide Vaccines. *Nat. Rev. Cancer* **2008**, *8*, 351−360.
(14) Yewdell, J. W. Designing CD8+ T Cell Vaccines: It's Not Rocket Science (Yet). *Curr. Opin. Immunol.* **2010**, *22*, 402−410.
(15) Mehta, N. K.; Moynihan, K. D.; Irvine, D. J. Engineering New Approaches to Cancer Vaccines. *Cancer Immunol. Res.* **2015**, *3*, 836−843.
(16) Eppler, H. B.; Jewell, C. M. Biomaterials as Tools to Decode Immunity. *Adv. Mater.* **2020**, *32*, No. 1903367.
(17) Feng, X.; Xu, W.; Li, Z.; Song, W.; Ding, J.; Chen, X. Immunomodulatory Nanosystems. *Adv. Sci. (Weinh)* **2019**, *6*, 1900101.
(18) Zhou, J.; Kroll, A. V.; Holay, M.; Fang, R. H.; Zhang, L. Biomimetic Nanotechnology toward Personalized Vaccines. *Adv. Mater.* **2020**, *32*, No. 1901255.
(19) Kuai, R.; Ochyl, L. J.; Bahjat, K. S.; Schwendeman, A.; Moon, J. J. Designer Vaccine Nanodiscs for Personalized Cancer Immunotherapy. *Nat. Mater.* **2017**, *16*, 489−496.
(20) Li, A. W.; Sobral, M. C.; Badrinath, S.; Choi, Y.; Graveline, A.; Stafford, A. G.; Weaver, J. C.; Dellacherie, M. O.; Shih, T. Y.; Ali, O. A.; Kim, J.; Wucherpfennig, K. W.; Mooney, D. J. A Facile Approach to Enhance Antigen Response for Personalized Cancer Vaccination. *Nat. Mater.* **2018**, *17*, 528.
(21) Luo, M.; Wang, H.; Wang, Z.; Cai, H.; Lu, Z.; Li, Y.; Du, M.; Huang, G.; Wang, C.; Chen, X.; Porembka, M. R.; Lea, J.; Frankel, A. E.; Fu, Y. X.; Chen, Z. J.; Gao, J. A STING-Activating Nanovaccine for Cancer Immunotherapy. *Nat. Nanotechnol.* **2017**, *12*, 648−654.
(22) Xu, C.; Nam, J.; Hong, H.; Xu, Y.; Moon, J. J. Positron Emission Tomography-Guided Photodynamic Therapy with Biodegradable Mesoporous Silica Nanoparticles for Personalized Cancer Immunotherapy. *ACS Nano* **2019**, *13*, 12148−12161.
(23) Zhu, G.; Mei, L.; Vishwasrao, H. D.; Jacobson, O.; Wang, Z.; Liu, Y.; Yung, B. C.; Fu, X.; Jin, A.; Niu, G.; Wang, Q.; Zhang, F.; Shroff, H.; Chen, X. Intertwining DNA-RNA Nanocapsules Loaded with Tumor Neoantigens as Synergistic Nanovaccines for Cancer Immunotherapy. *Nat. Commun.* **2017**, *8*, 1482.
(24) Lynn, G. M.; Sedlik, C.; Baharom, F.; Zhu, Y.; Ramirez-Valdez, R. A.; Coble, V. L.; Tobin, K.; Nichols, S. R.; Itzkowitz, Y.; Zaidi, N.; Gammon, J. M.; Blobel, N. J.; Denizeau, J.; de la Rochere, P.; Francica, B. J.; Decker, B.; Maciejewski, M.; Cheung, J.; Yamane, H.; Smelkinson, M. G. Peptide-TLR-7/8a Conjugate Vaccines Chemically Programmed for Nanoparticle Self-Assembly Enhance CD8 T-Cell Immunity to Tumor Antigens. *Nat. Biotechnol.* **2020**, *38*, 320.
(25) Woo, S. R.; Corrales, L.; Gajewski, T. F. The STING Pathway and the T Cell-Inflamed Tumor Microenvironment. *Trends Immunol.* **2015**, *36*, 250−256.
(26) Woo, S. R.; Fuertes, M. B.; Corrales, L.; Spranger, S.; Furdyna, M. J.; Leung, M. Y.; Duggan, R.; Wang, Y.; Barber, G. N.; Fitzgerald, K. A.; Alegre, M. L.; Gajewski, T. F. STING-Dependent Cytosolic DNA Sensing Mediates Innate Immune Recognition of Immunogenic Tumors. *Immunity* **2014**, *41*, 830−842.
(27) Deng, L.; Liang, H.; Xu, M.; Yang, X.; Burnette, B.; Arina, A.; Li, X. D.; Mauceri, H.; Beckett, M.; Darga, T.; Huang, X.; Gajewski, T. F.; Chen, Z. J.; Fu, Y. X.; Weichselbaum, R. R. STING-Dependent Cytosolic DNA Sensing Promotes Radiation-Induced Type I Interferon-Dependent Antitumor Immunity in Immunogenic Tumors. *Immunity* **2014**, *41*, 843−852.
(28) Fu, J.; Kanne, D. B.; Leong, M.; Glickman, L. H.; McWhirter, S. M.; Lemmens, E.; Mechette, K.; Leong, J. J.; Lauer, P.; Liu, W.; Sivick, K. E.; Zeng, Q.; Soares, K. C.; Zheng, L.; Portnoy, D. A.; Woodward, J. J.; Pardoll, D. M.; Dubensky, T. W., Jr.; Kim, Y. STING Agonist Formulated Cancer Vaccines Can Cure Established Tumors Resistant to PD-1 Blockade. *Sci. Transl. Med.* **2015**, *7*, 283ra52.
(29) Kinkead, H. L.; Hopkins, A.; Lutz, E.; Wu, A. A.; Yarchoan, M.; Cruz, K.; Woolman, S.; Vithayathil, T.; Glickman, L. H.; Ndubaku, C. O.; McWhirter, S. M.; Dubensky, T. W., Jr.; Armstrong, T. D.; Jaffee, E. M.; Zaidi, N. Combining STING-Based Neoantigen-Targeted Vaccine with Checkpoint Modulators Enhances Antitumor Immunity in Murine Pancreatic Cancer. *JCI Insight* **2018**, *3*, e122857.
(30) Gutjahr, A.; Papagno, L.; Nicoli, F.; Kanuma, T.; Kuse, N.; Cabral-Piccin, M. P.; Rochereau, N.; Gostick, E.; Lioux, T.; Perouzel, E.; Price, D. A.; Takiguchi, M.; Verrier, B.; Yamamoto, T.; Paul, S.; Appay, V. The STING Ligand cGAMP Potentiates the Efficacy of Vaccine-Induced CD8+ T Cells. *JCI Insight* **2019**, *4*, e125107.
(31) Wang, Z.; Celis, E. STING Activator C-Di-Gmp Enhances the Anti-Tumor Effects of Peptide Vaccines in Melanoma-Bearing Mice. *Cancer Immunol. Immunother.* **2015**, *64*, 1057−1066.
(32) Chandra, D.; Quispe-Tintaya, W.; Jahangir, A.; Asafu-Adjei, D.; Ramos, I.; Sintim, H. O.; Zhou, J.; Hayakawa, Y.; Karaolis, D. K.; Gravekamp, C. STING Ligand C-Di-Gmp Improves Cancer Vaccination against Metastatic Breast Cancer. *Cancer Immunol. Res.* **2014**, *2*, 901−910.
(33) Irvine, D. J.; Swartz, M. A.; Szeto, G. L. Engineering Synthetic Vaccines Using Cues from Natural Immunity. *Nat. Mater.* **2013**, *12*, 978−990.
(34) Swartz, M. A.; Hirosue, S.; Hubbell, J. A. Engineering Approaches to Immunotherapy. *Sci. Transl. Med.* **2012**, *4*, 148rv9.
(35) Liu, H.; Moynihan, K. D.; Zheng, Y.; Szeto, G. L.; Li, A. V.; Huang, B.; Van Egeren, D. S.; Park, C.; Irvine, D. J. Structure-Based Programming of Lymph-Node Targeting in Molecular Vaccines. *Nature* **2014**, *507*, 519−522.
(36) Dubensky, T. W., Jr.; Kanne, D. B.; Leong, M. L. Rationale, Progress and Development of Vaccines Utilizing STING-Activating Cyclic Dinucleotide Adjuvants. *Ther. Adv. Vaccines* **2013**, *1*, 131−143.
(37) Hanson, M. C.; Crespo, M. P.; Abraham, W.; Moynihan, K. D.; Szeto, G. L.; Chen, S. H.; Melo, M. B.; Mueller, S.; Irvine, D. J. Nanoparticulate STING Agonists Are Potent Lymph Node-Targeted Vaccine Adjuvants. *J. Clin. Invest.* **2015**, *125*, 2532−2546.
(38) Shae, D.; Becker, K. W.; Christov, P.; Yun, D. S.; Lytton-Jean, A. K. R.; Sevimli, S.; Ascano, M.; Kelley, M.; Johnson, D. B.; Balko, J. M.; Wilson, J. T. Endosomolytic Polymersomes Increase the Activity of Cyclic Dinucleotide STING Agonists to Enhance Cancer Immunotherapy. *Nat. Nanotechnol.* **2019**, *14*, 269−278.
(39) Hubbell, J. A.; Swartz, M. A. Trojan Horses for Immunotherapy. *Nat. Nanotechnol.* **2019**, *14*, 196−197.
(40) Koshy, S. T.; Cheung, A. S.; Gu, L.; Graveline, A. R.; Mooney, D. J. Liposomal Delivery Enhances Immune Activation by STING

https://dx.doi.org/10.1021/acsnano.0c02765
ACS Nano 2020, 14, 9904−9916

Agonists for Cancer Immunotherapy. *Advanced Biosystems* **2017**, *1*, 1600013.
(41) Cheng, N.; Watkins-Schulz, R.; Junkins, R. D.; David, C. N.; Johnson, B. M.; Montgomery, S. A.; Peine, K. J.; Darr, D. B.; Yuan, H.; McKinnon, K. P.; Liu, Q.; Miao, L.; Huang, L.; Bachelder, E. M.; Ainslie, K. M.; Ting, J. P. A Nanoparticle-Incorporated STING Activator Enhances Antitumor Immunity in PD-L1-Insensitive Models of Triple-Negative Breast Cancer. *JCI Insight* **2018**, *3*, e120638.
(42) Nakamura, T.; Miyabe, H.; Hyodo, M.; Sato, Y.; Hayakawa, Y.; Harashima, H. Liposomes Loaded with a STING Pathway Ligand, Cyclic Di-Gmp, Enhance Cancer Immunotherapy against Metastatic Melanoma. *J. Controlled Release* **2015**, *216*, 149−157.
(43) Liu, Y.; Crowe, W. N.; Wang, L.; Lu, Y.; Petty, W. J.; Habib, A. A.; Zhao, D. An Inhalable Nanoparticulate STING Agonist Synergizes with Radiotherapy to Confer Long-Term Control of Lung Metastases. *Nat. Commun.* **2019**, *10*, 5108.
(44) Wang, J.; Li, P.; Yu, Y.; Fu, Y.; Jiang, H.; Lu, M.; Sun, Z.; Jiang, S.; Lu, L.; Wu, M. X. Pulmonary Surfactant-Biomimetic Nanoparticles Potentiate Heterosubtypic Influenza Immunity. *Science* **2020**, *367*, eaau0810.
(45) Lin, L. C.; Huang, C. Y.; Yao, B. Y.; Lin, J. C.; Agrawal, A.; Algaissi, A.; Peng, B. H.; Liu, Y. H.; Huang, P. H.; Juang, R. H.; Chang, Y. C.; Tseng, C. T.; Chen, H. W.; Hu, C. J. Viromimetic STING Agonist-Loaded Hollow Polymeric Nanoparticles for Safe and Effective Vaccination against Middle East Respiratory Syndrome Coronavirus. *Adv. Funct. Mater.* **2019**, *29*, 1807616.
(46) Wilson, D. R.; Sen, R.; Sunshine, J. C.; Pardoll, D. M.; Green, J. J.; Kim, Y. J. Biodegradable STING Agonist Nanoparticles for Enhanced Cancer Immunotherapy. *Nanomedicine* **2018**, *14*, 237−246.
(47) An, M.; Yu, C.; Xi, J.; Reyes, J.; Mao, G.; Wei, W. Z.; Liu, H. Induction of Necrotic Cell Death and Activation of STING in the Tumor Microenvironment *via* Cationic Silica Nanoparticles Leading to Enhanced Antitumor Immunity. *Nanoscale* **2018**, *10*, 9311−9319.
(48) Ahn, J.; Xia, T.; Rabasa Capote, A.; Betancourt, D.; Barber, G. N. Extrinsic Phagocyte-Dependent STING Signaling Dictates the Immunogenicity of Dying Cells. *Cancer Cell* **2018**, *33*, 862−873.
(49) Kitai, Y.; Kawasaki, T.; Sueyoshi, T.; Kobiyama, K.; Ishii, K. J.; Zou, J.; Akira, S.; Matsuda, T.; Kawai, T. DNA-Containing Exosomes Derived from Cancer Cells Treated with Topotecan Activate a STING-Dependent Pathway and Reinforce Antitumor Immunity. *J. Immunol.* **2017**, *198*, 1649−1659.
(50) Kwon, J.; Bakhoum, S. F. The Cytosolic DNA-Sensing cGAS-STING Pathway in Cancer. *Cancer Discovery* **2020**, *10*, 26.
(51) Manicassamy, S.; Pulendran, B. Dendritic Cell Control of Tolerogenic Responses. *Immunol Rev.* **2011**, *241*, 206−227.
(52) Audiger, C.; Rahman, M. J.; Yun, T. J.; Tarbell, K. V.; Lesage, S. The Importance of Dendritic Cells in Maintaining Immune Tolerance. *J. Immunol.* **2017**, *198*, 2223−2231.
(53) Knight, F. C.; Gilchuk, P.; Kumar, A.; Becker, K. W.; Sevimli, S.; Jacobson, M. E.; Suryadevara, N.; Wang-Bishop, L.; Boyd, K. L.; Crowe, J. E.; Joyce, S.; Wilson, J. T. Mucosal Immunization with a pH-Responsive Nanoparticle Vaccine Induces Protective CD8+ Lung-Resident Memory T Cells. *ACS Nano* **2019**, *13*, 10939−10960.
(54) Qiu, F.; Becker, K. W.; Knight, F. C.; Baljon, J. J.; Sevimli, S.; Shae, D.; Gilchuk, P.; Joyce, S.; Wilson, J. T. Poly(propylacrylic Acid)-Peptide Nanoplexes as a Platform for Enhancing the Immunogenicity of Neoantigen Cancer Vaccines. *Biomaterials* **2018**, *182*, 82−91.
(55) Thomas, S. N.; Schudel, A. Overcoming Transport Barriers for Interstitial-, Lymphatic-, and Lymph Node-Targeted Drug Delivery. *Curr. Opin. Chem. Eng.* **2015**, *7*, 65−74.
(56) Lirussi, D.; Ebensen, T.; Schulze, K.; Trittel, S.; Duran, V.; Liebich, I.; Kalinke, U.; Guzman, C. A. Type I IFN and Not TFN, Is Essential for Cyclic Di-Nucleotide-Elicited CTL by a Cytosolic Cross-Presentation Pathway. *EBioMedicine* **2017**, *22*, 100−111.
(57) Wang, H.; Hu, S.; Chen, X.; Shi, H.; Chen, C.; Sun, L.; Chen, Z. J. cGAS Is Essential for the Antitumor Effect of Immune Checkpoint Blockade. *Proc. Natl. Acad. Sci. U. S. A.* **2017**, *114*, 1637−1642.
(58) Reddy, S. T.; van der Vlies, A. J.; Simeoni, E.; Angeli, V.; Randolph, G. J.; O'Neil, C. P.; Lee, L. K.; Swartz, M. A.; Hubbell, J. A. Exploiting Lymphatic Transport and Complement Activation in Nanoparticle Vaccines. *Nat. Biotechnol.* **2007**, *25*, 1159−1164.
(59) Yadav, M.; Jhunjhunwala, S.; Phung, Q. T.; Lupardus, P.; Tanguay, J.; Bumbaca, S.; Franci, C.; Cheung, T. K.; Fritsche, J.; Weinschenk, T.; Modrusan, Z.; Mellman, I.; Lill, J. R.; Delamarre, L. Predicting Immunogenic Tumour Mutations by Combining Mass Spectrometry and Exome Sequencing. *Nature* **2014**, *515*, 572−576.
(60) Ott, P. A.; Hu, Z.; Keskin, D. B.; Shukla, S. A.; Sun, J.; Bozym, D. J.; Zhang, W.; Luoma, A.; Giobbie-Hurder, A.; Peter, L.; Chen, C.; Olive, O.; Carter, T. A.; Li, S.; Lieb, D. J.; Eisenhaure, T.; Gjini, E.; Stevens, J.; Lane, W. J.; Javeri, I.; et al. An Immunogenic Personal Neoantigen Vaccine for Patients with Melanoma. *Nature* **2017**, *547*, 217−221.
(61) Taylor, M. A.; Hughes, A. M.; Walton, J.; Coenen-Stass, A. M. L.; Magiera, L.; Mooney, L.; Bell, S.; Staniszewska, A. D.; Sandin, L. C.; Barry, S. T.; Watkins, A.; Carnevalli, L. S.; Hardaker, E. L. Longitudinal Immune Characterization of Syngeneic Tumor Models to Enable Model Selection for Immune Oncology Drug Discovery. *J. Immunother Cancer* **2019**, *7*, 328.
(62) Kourtis, I. C.; Hirosue, S.; de Titta, A.; Kontos, S.; Stegmann, T.; Hubbell, J. A.; Swartz, M. A. Peripherally Administered Nanoparticles Target Monocytic Myeloid Cells, Secondary Lymphoid Organs and Tumors in Mice. *PLoS One* **2013**, *8*, No. e61646.
(63) Zhang, F.; Stephan, S. B.; Ene, C. I.; Smith, T. T.; Holland, E. C.; Stephan, M. T. Nanoparticles That Reshape the Tumor Milieu Create a Therapeutic Window for Effective T-Cell Therapy in Solid Malignancies. *Cancer Res.* **2018**, *78*, 3718−3730.
(64) Kranz, L. M.; Diken, M.; Haas, H.; Kreiter, S.; Loquai, C.; Reuter, K. C.; Meng, M.; Fritz, D.; Vascotto, F.; Hefesha, H.; Grunwitz, C.; Vormehr, M.; Husemann, Y.; Selmi, A.; Kuhn, A. N.; Buck, J.; Derhovanessian, E.; Rae, R.; Attig, S.; Diekmann, J.; et al. Systemic RNA Delivery to Dendritic Cells Exploits Antiviral Defence for Cancer Immunotherapy. *Nature* **2016**, *534*, 396−401.
(65) Kreiter, S.; Vormehr, M.; van de Roemer, N.; Diken, M.; Lower, M.; Diekmann, J.; Boegel, S.; Schrors, B.; Vascotto, F.; Castle, J. C.; Tadmor, A. D.; Schoenberger, S. P.; Huber, C.; Tureci, O.; Sahin, U. Mutant MHC Class II Epitopes Drive Therapeutic Immune Responses to Cancer. *Nature* **2015**, *520*, 692−696.
(66) Hilf, N.; Kuttruff-Coqui, S.; Frenzel, K.; Bukur, V.; Stevanovic, S.; Gouttefangeas, C.; Platten, M.; Tabatabai, G.; Dutoit, V.; van der Burg, S. H.; Thor Straten, P.; Martinez-Ricarte, F.; Ponsati, B.; Okada, H.; Lassen, U.; Admon, A.; Ottensmeier, C. H.; Ulges, A.; Kreiter, S.; von Deimling, A.; et al. Actively Personalized Vaccination Trial for Newly Diagnosed Glioblastoma. *Nature* **2019**, *565*, 240−245.
(67) Temizoz, B.; Kuroda, E.; Ohata, K.; Jounai, N.; Ozasa, K.; Kobiyama, K.; Aoshi, T.; Ishii, K. J. TLR9 and STING Agonists Synergistically Induce Innate and Adaptive Type II IFN. *Eur. J. Immunol.* **2015**, *45*, 1159−1169.
(68) Atukorale, P. U.; Raghunathan, S. P.; Raguveer, V.; Moon, T. J.; Zheng, C.; Bielecki, P. A.; Wiese, M. L.; Goldberg, A. L.; Covarrubias, G.; Hoimes, C. J.; Karathanasis, E. Nanoparticle Encapsulation of Synergistic Immune Agonists Enables Systemic Codelivery to Tumor Sites and IFN -Driven Antitumor Immunity. *Cancer Res.* **2019**, *79*, 5394−5406.
(69) Collier, M. A.; Junkins, R. D.; Gallovic, M. D.; Johnson, B. M.; Johnson, M. M.; Macintyre, A. N.; Sempowski, G. D.; Bachelder, E. M.; Ting, J. P.; Ainslie, K. M. Acetalated Dextran Microparticles for Codelivery of STING and TLR7/8 Agonists. *Mol. Pharmaceutics* **2018**, *15*, 4933−4946.
(70) Gaffney, B. L.; Veliath, E.; Zhao, J.; Jones, R. A. One-Flask Syntheses of C-Di-Gmp and the [Rp,Rp] and [Rp,Sp] Thiophosphate Analogues. *Org. Lett.* **2010**, *12*, 3269−3271.
(71) Karttunen, J.; Sanderson, S.; Shastri, N. Detection of Rare Antigen-Presenting Cells by the Lacz T-Cell Activation Assay

https://dx.doi.org/10.1021/acsnano.0c02765
ACS Nano 2020, 14, 9904−9916

Suggests an Expression Cloning Strategy for T-Cell Antigens. *Proc. Natl. Acad. Sci. U. S. A.* **1992**, *89*, 6020−6024.

https://dx.doi.org/10.1021/acsnano.0c02765
ACS Nano 2020, 14, 9904−9916